Bring me a shrubbery! Distinguishing herbaceous and woody vegetation in the Lower Amazon floodplain using Landsat TM imagery

Katrina Waechter
katrina.waechter@du.edu
University of Denver

Advanced Remote Sensing
Spring 2014

Abstract. The mapping of non-forest vegetation in the Amazon River floodplain remains a challenge to land use studies. A method to classification of non-forest vegetation using multi-date optical satellite imagery is needed. This paper explores the use of a ratio of pure spectral materials to distinguish between herbaceous and woody non-forest vegetation. Spectral mixture analysis is applied to Landsat 5TM scenes from the Lower Amazon floodplain. A ratio of green vegetation to non-photosynthetic vegetation fractions of pixels is calculated and used with shade fractions per pixel to identify potential thresholds for classification. Mid-level water stage yields most reasonable endmember fractions and fraction ratio. At mid-level water, Landsat 5 TM Climate Data Record surface reflectance is noticeably different fractions and ratio than ENVI FLAASH corrected surface reflectance. Results from both correction methods are similar and do not cause significant difference in woody and herbaceous vegetation separability. The endmember fraction ratio shows potential for use in land cover classification, but cannot separate herbaceous and woody non-forest vegetation beyond subtle and variable fraction ratio and shade fraction thresholds.

Keywords: remote sensing, Amazon, varzea, land cover, non-forest vegetation, Spectral Mixture Analysis

1. Introduction

The floodplain (varzea) of the main stem Amazon River is one of the largest riverine wetlands in the world, comprised of complex and dynamic landforms in a mosaic of permanent and seasonal lakes, channels, levees, and flats. The varzea houses unique flora and fauna and provides riverside communities with critical ecosystem services. Dominant economic activities in the area include commercial fishing and livestock grazing, the impacts of which are causing habitat degradation (McGrath et al. 2007). In order to understand long-term impacts of increased economic activity (e.g., increased cattle density, overfishing), particularly habitat degradation and deforestation, a detailed mapping of land cover in the varzea is needed. The main stem Amazon River varzea is covered by a variety of vegetation physiognomies, including terrestrial and aquatic herbaceous, shrub, and trees. The varzea occupy a smaller total area compared to the upland forests, but their contributions to biodiversity and ecosystem services are greater than upland forests (Martinez and LeToan 2007). Forested areas of the lower varzea have decreased 13 percent since the 1970s while other land cover surfaces, such as non-forest vegetation and bare soil, have increased (Réno et al. 2011).

Land cover surface extent must be known before assessment of impacts of past and current land cover change to communities and biodiversity. Flood extent and vegetation structure in the varzea can be efficiently mapped using synthetic aperture radar (Hess et al. 2003), but only optical imagery is available for multi-decadal range in the varzea. Forests can be consistently mapped using multiple methods with optical imagery, but ability to classify non-forest vegetation in the varzea has been limited by availability of cloud-free scenes and sensor resolution. The purpose of this project is to evaluate the utility of an application of Spectral Mixture Analysis (SMA) to distinguish between herbaceous and woody non-forest vegetation in the varzea.

2. Study Area

The study focuses on a portion of the varzea at the western edge of the state of Para, centered on the cities of Obidos and Oriximina as well as the confluence of the Amazon and Trombetas Rivers. There are four main landscape elements: the main river channel, natural levees, permanent lakes, and seasonally inundated grasslands. Great seasonal variability in temporal and spatial distribution of annual flooding, also known as the "flood pulse", drives productivity, biodiversity, and biogeochemistry in the varzea by flood amplitude and periodicity (Junk et al. 1989). Figure 1 frames the study area and highlights the difference in vegetation and land cover between falling water (upper left) and low water stages (lower right). This area of the varzea is home to more than 30 small agro-extractivist communities (30-100+ households) separated by ranches (de Castro 2003).

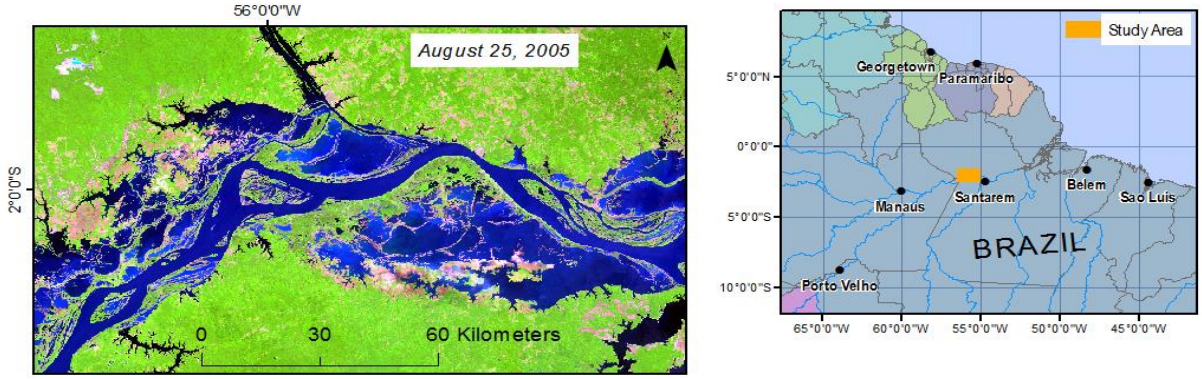

Figure 1. False color RGB (Bands 5, 4, 3) composites of Landsat 5 TM scenes from the Amazon main stem study area with regional inset (upper right)

3. Methodology

The driving concept behind this study is to test whether an endmember fraction ratio of main spectral constituents (green vegetation and non-photosynthetic vegetation) could distinguish between herbaceous and woody non-forest vegetation in the study area. Scenes from a medium resolution multispectral sensor were used to retain proportion of mixed pixels and avoid increased spectral variability of endmembers (Wu 2004). Six Landsat 5 TM scenes (path 228 and rows 61 and 62) from three dates of varying water levels were used to test a vegetation endmember fraction ratio. Landsat Surface Reflectance Climate Data Record (CDR) scenes were used to reduce processing time and to compare against the ENVI FLAASH atmospheric corrected scene used to compile the spectral library used in this project. CDR scenes of the same date (8/25/2005, 10/28/2005, 9/5/2009 respectively) were subset and mosaicked to match the spatial extent of the Landsat 5 TM scene (8/25/2005) used to collect the project spectral library. Linear stretch of 4% was applied to Row 62 scenes to match color and contrast of Row 61 scenes.

Using bands 1-5 and 7, spectral mixture analysis using two-, three-, and four-endmember models was applied for each of the scene dates in various combinations. Endmember fractions were constrained to (-.05-1.05) and no constraint was placed on RMS error. The project spectral library, including sand, silt, non-photosynthetic vegetation (NPV), and green vegetation (GV) spectra, was iteratively selected from dominant land cover components and tested using FLAASH-corrected Landsat 5 TM surface reflectance scenes (Powell et al. 2014). From each endmember model, endmember fraction ratios were computed by dividing GV fraction by NPV fraction. Fraction ratios from three-endmember and four-endmember models did not provide sufficient difference to distinguish structural or phenological differences between vegetation. However, fraction ratios derived from two-endmember models (vegetation type and photometric shade) provided sufficient difference to visually identify forest and non-forest vegetation. To increase difference in the fraction ratio, a squared transformation was applied to each fraction ratio.

4. Results and Discussion

Fraction ratios between different water levels as well as to a detailed classification map of an alluvial island near the community of Magdalena (Figure 2) were qualitatively compared. Fraction ratios did not vary significantly during higher water (9/5/2009) and are likely too far removed temporally to compare. Fraction ratios varied substantially enough in the falling- and low-water stages in 2005 scenes. However, too many pixels in the low-water stage scene (10/28/2005) were unmodeled (11%) by the two-endmember mixture model to warrant further application of the fraction ratio without changes.

To maintain spectral integrity with the project spectral library, endmember fraction ratios from both the ENVI FLAASH-corrected and CDR scenes were tested for distinguishability of different land covers as detailed by de Menezes (2011). Figure 2 shows how FLAASH (2D plot, right) and CDR (2D plot, left) derived fractions plotted by photometric shade can be preliminarily distinguished, abiding by similar symbology as the known land cover from 1995. There is substantial confusion between water (blue) and soil (red) as well as between forest (dark green) and shrub (light green), but terrestrial grasses (yellow) as well as macrophytes and aningais (cyan) are distinguishable.

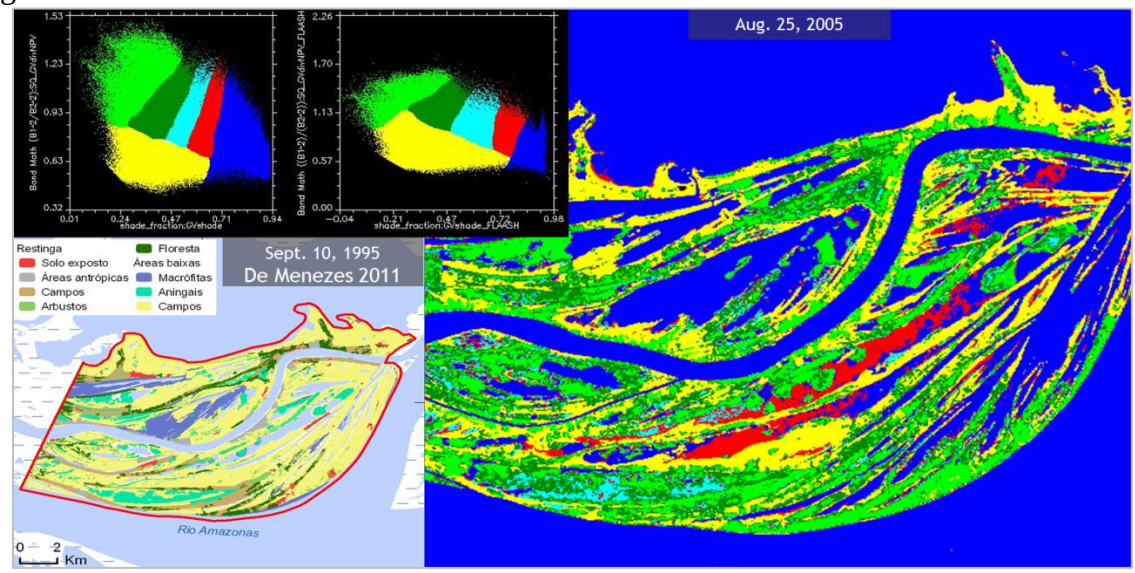

Figure 2. Qualitative comparison of density slice map (right) derived from CDR reflectance and FLAASH reflectance using 2D scatterplot of GV/NPV ratio (Y) and shade fraction (X) against participatory land cover classification (bottom left)

While density slice maps can be created to best fit local subset conditions, land cover thresholds of fraction ratio and shade fraction are not consistent with the floodplain using this method. The range of the endmember fraction ratio from FLAASH corrected reflectance is wider than CDR reflectance, but both correction methods create similar, skewed plots of fraction ratio and shade fraction.

5. Conclusions

The use of a green vegetation to non-photosynthetic vegetation endmember fraction ratio shows potential for use in distinguishing herbaceous and woody non-forest vegetation in the varzea but requires refinement, particularly if using CDR reflectance. Figure 3 illustrates the separability of land cover types of interest by correction method in average fraction ratio and shade fraction. In the future, the use of endmember fraction ratios and shade fraction in principal component analysis may be explored. Furthermore, the use of three-endmember models needs to be explored to reduce RMSE and model soil constituents.

Vegetation Endmember Fraction Ratio and Shade Fraction by Atmospheric Correction Method

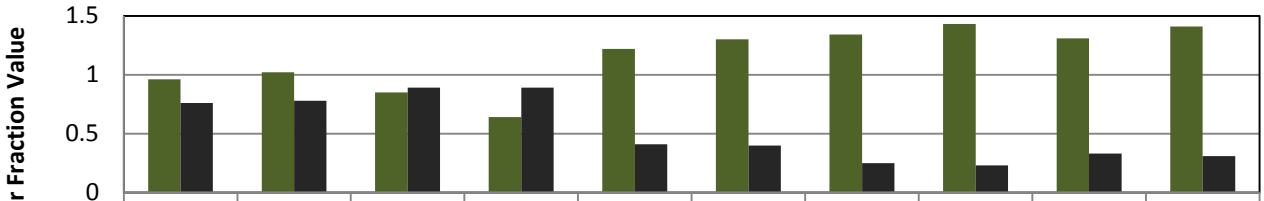

	Bright Water (CDR)	Bright Water (FLAASH)	Dark Water (CDR)	Dark Water (FLAASH)	Forest (CDR)	Forest (FLAASH)	Macrophyte (CDR)	Macrophyte (FLAASH)	Shrub (CDR)	Shrub (FLAASH)
GV/NPV Ratio	0.96	1.02	0.85	0.64	1.22	1.3	1.34	1.43	1.31	1.41
Shade Fraction	0.76	0.78	0.89	0.89	0.41	0.4	0.25	0.23	0.33	0.31

Figure 3. Comparison of endmember fraction ratio and shade fraction between land cover classes of interest

6. References

de Castro, F. & McGrath, D. G. (2003). Moving Toward Sustainability in the Local Management of Floodplain Lake Fisheries in the Brazilian Amazon. Human Organization, 62(2), 123-133.

Hess, L. L., Melack, J. M., Novo, E. M. L. M., Barbosa, C. C. F., & Gastil, M. (2003). Dual-season mapping of wetland inundation and vegetation for the central Amazon basin. Remote Sensing of Environment, 87(2003), 404-428.

Junk, W. J., Bayley, P. B., & Sparks, R. E. (1989). The flood pulse concept in the river-floodplain systems. Canadian Special Publication in Fisheries and Aquatic Sciences, 106(1989), 110-127.

Martinez, J. M. & Le Toan, T. (2007). Mapping of flood dynamics and spatial distribution of vegetation in the Amazon floodplain using multitemporal SAR data. Remote Sensing of Environment, 108(2007), 209-223.

McGrath, D. G., Almeida, O. T., & Merry, F. D. (2007). The Influence of Community Management Agreements on Household Economic Strategies: Cattle Grazing and Fishing Agreements of the Lower Amazon Floodplain. International Journal of the Commons, 1(1), 67-87.

de Menezes, D. P. (2011). Thematic Mapping in the Lower Amazon's Floodplain. IPAM, accessed February 4, available at www.ipam.org.br/revista/imprimir/312.

Powell, R. L., Hess, L. L., Silva, T. F., Isherwood, J., & McGrath, D. (2014). Inter- and intra-annual characterization of Amazon floodplain habitats with multiple endmember spectral mixture analysis. Paper presented at the annual meeting of the American Association of Geographers, Tampa, Florida, April 19-25.

Reno, V. F., Novo, E. M., Suemitsu, C., Renno, C. D., & Silva, T. S. (2011). Assessment of deforestation in the Lower Amazon floodplain using historical Landsat MSS/TM imagery. Remote Sensing of Environment, 115(12), 3446-3456.

Wu, C. (2009). Quantifying high-resolution impervious surfaces using spectral mixture analysis. International Journal of Remote Sensing, 30(11), 2915-2932.